CVI
Journals.ASM.org

# Characterization and Epitope Mapping of the Polyclonal Antibody Repertoire Elicited by Ricin Holotoxin-Based Vaccination

**Ofer Cohen,[a] Adva Mechaly,[b] Tamar Sabo,[a] Ron Alcalay,[a] Ronit Aloni-Grinstein,[a] Nehama Seliger,[a] Chanoch Kronman,[a] Ohad Mazor[a]**

Departments of Biochemistry and Molecular Genetics[a] and Infectious Diseases,[b] Israel Institute for Biological Research, Ness-Ziona, Israel

**Ricin, one of the most potent and lethal toxins known, is classified by the Centers for Disease Control and Prevention (CDC) as a select agent. Currently, there is no available antidote against ricin exposure, and the most promising therapy is based on neutralizing antibodies elicited by active vaccination or that are given passively. The aim of this study was to characterize the repertoire of anti-ricin antibodies generated in rabbits immunized with ricin toxoid. These anti-ricin antibodies exhibit an exceptionally high avidity (thiocyanate-based avidity index, 9 M) toward ricin and an apparent affinity of 1 nM. Utilizing a novel tissue culture-based assay that enables the determination of ricin activity within a short time period, we found that the anti-ricin antibodies also possess a very high neutralizing titer. In line with these findings, these antibodies conferred mice with full protection against pulmonary ricinosis when administered as a passive vaccination. Epitope mapping analysis using phage display random peptide libraries revealed that the polyclonal serum contains four immunodominant epitopes, three of which are located on the A subunit and one on the B subunit of ricin. Only two of the four epitopes were found to have a significant role in ricin neutralization. To the best of our knowledge, this is the first work that characterizes these immunological aspects of the polyclonal response to ricin holotoxin-based vaccination. These findings provide useful information and a possible strategy for the development and design of an improved ricin holotoxin-based vaccine.**

Ricin, derived from the plant *Ricinus communis*, is one of the most lethal toxins known. The toxin consists of two covalently linked subunits: the A subunit (RTA) is an *N*-glycosidase that irreversibly inactivates the 28S rRNA of the mammalian 60S ribosome subunit, and the B subunit (RTB) is a galactose-specific lectin that mediates the binding of the toxin to the cell membrane (1). The high toxicity, availability, and ease of production and dissemination of ricin render it an attractive tool for bioterrorism, and ricin was therefore classified as a category B select agent by the Centers for Disease Control and Prevention (CDC). Currently, there is no available antidote against ricin exposure, underlining the need to develop effective countermeasures. Numerous efforts have been made to identify small molecules that inhibit the catalytic activity of RTA (2, 3) in order to develop aptamers or sugar analogs that prevent the binding of ricin to the cell membrane (4, 5) or to inhibit the intracellular trafficking of the toxin (6). While several of these studies demonstrated an inhibitory effect of ricin activity *in vitro*, they were not as effective *in vivo*. To date, the most promising antiricin therapy is based on neutralizing antibodies elicited by active vaccination or that are given passively. Over a decade ago, several research programs were initiated that aimed to develop an effective RTA-based vaccine (7). However, the prophylactic immunization of large populations (civilians, military personnel, or first responders) to protect them from ricin exposure is of limited scope, while antibody-based passive vaccination seems to be of greater relevance to the general public. Indeed, it was shown that the administration of ricin-neutralizing antibodies can provide protection from ricin toxicity (8–11). Moreover, we recently demonstrated that a combined treatment of doxycycline and highly potent anti-ricin polyclonal antibodies results in improved survival rates of ricin-intoxicated mice (12).

While for many years it was thought that RTB rarely induces a protective antibody response, recent studies have challenged this notion and suggested that a holotoxin vaccination should be considered (11, 13–15). A ricin toxoid-based vaccine, prepared by treating the toxin with formaldehyde (which enables the retention of the protein original secondary structure [16]), was shown before to induce high titers of protective antibodies (17). As part of an ongoing effort to develop a vaccination strategy that will induce high titers of ricin-neutralizing antibodies to be used for passive immunization, we set out to characterize the repertoire of the anti-ricin antibodies generated following immunization with ricin toxoid.

Epitope mapping of the polyclonal antibodies in the sera of immunized animals is used as a tool for discovering the antigenic moieties of pathogens, and it provides important information for the development of vaccines (18–22). Yet, the few studies that have sought to map the polyclonal response toward ricin have used only RTA as the immunogenic entity (23, 24). We have therefore performed, as part of this study, an epitope mapping analysis of the anti-ricin antibodies in order to identify the immunodominant epitopes in both ricin subunits and to determine the roles of these epitopes in ricin neutralization.

## MATERIALS AND METHODS

**Antibodies and reagents.** Pure ricin was prepared as described previously (12). To obtain RTA and RTB, ricin was reduced in the presence of 50 mM dithiothreitol and 100 mM iodoacetamide in Tris-HCl (pH 9.0), dialyzed against phosphate-buffered saline (PBS), and loaded onto a lactamyl-agarose gel while collecting the unbound RTA. RTB was eluted using 0.5 M galactose and then dialyzed against PBS. *Ulex europaeus*, alkaline phos-

Received 28 July 2014 Returned for modification 27 August 2014
Accepted 6 September 2014
Published ahead of print 10 September 2014
Editor: S. A. Plotkin
Address correspondence to Ohad Mazor, ohadm@iibr.gov.il.

doi:10.1128/CVI.00510-14

phatase-conjugated secondary antibodies, and *p*-nitrophenyl phosphate (PNPP) were obtained from Sigma-Aldrich. Anti-M13-horseradish peroxidase (HRP)-conjugated antibody was purchased from GE Healthcare (Sweden) and 3,3′,5,5′-tetramethylbenzidine (TMB-E) from the Millipore Corporation (USA).

**Animal studies.** All animal experiments were performed in accordance with the Israeli law and were approved by the ethics committee for animal experiments at the Israel Institute for Biological Research. Mice (CD1) were obtained from Charles River Laboratories (England). New Zealand White rabbits (2.5 to 3 kg) were obtained from Charles River Laboratories (Wilmington, MA). The animals were maintained at 20 to 22°C and a relative humidity of 50% ± 10% on a 12-h light/dark cycle, fed with commercial rodent chow (Koffolk, Inc.), and provided with tap water *ad libitum*. The treatment of animals was in accordance with regulations outlined in the USDA Animal Welfare Act and the conditions specified in the Guide for care and use of laboratory animals (25).

**Anti-ricin antibodies.** Ricin toxoid was prepared by incubating ricin in 4.2% formaldehyde for the first 18 h at 47°C and then incubating it for another 30 h at 42°C, followed by an extensive dialysis against double-distilled water ($ddH_2O$). Three rabbits were immunized with ricin toxoid that was emulsified with complete Freund's adjuvant, followed by four monthly booster injections of ricin toxoid emulsified with incomplete Freund's adjuvant. The preparation and purification of the pooled IgG fraction of the polyclonal anti-ricin antibodies derived from the immunized rabbits were performed as described before (12). To purify the ricin-binding antibody fraction, ricin was covalently linked to a beaded agarose gel using the AminoLink coupling kit (Thermo Scientific, USA). The polyclonal antibodies were loaded on the column, and following a wash step, the ricin-specific antibodies were eluted and collected.

***In vitro* ricin neutralization assay.** HEK293-acetylcholinesterase (AChE) cells (26) were cultured in Dulbecco's modified Eagle's medium (DMEM) (Biological Industries, Beit Haemek, Israel) supplemented with 10% fetal calf serum (FCS). For the cytotoxicity studies, the cells were seeded in 96-well plates ($1 \times 10^5$ cells/well) in medium containing ricin (2 ng/ml) in the presence or absence of anti-ricin antibodies. Sixteen hours later, the medium was replaced, the cells were incubated for 2 h, and the amount of secreted AChE in each well was assayed according to Ellman et al. (27) in the presence of 0.1 mg/ml bovine serum albumin (BSA), 0.3 mM 5,5′-dithiobis(2-nitrobenzoic acid), 50 mM sodium phosphate buffer (pH 8.0), and 0.5 mM acetylthiocholine iodide (ATC). In order to determine the inhibitory effect of selected phages on the neutralizing activity of the anti-ricin antibodies, ricin (2 ng/ml) was preincubated with a fixed amount of antibodies and phages ($1 \times 10^{12}$), and the assay was continued as described above.

**Enzyme-linked immunosorbent assay.** MaxiSorp 96-well microtiter plates (Nunc, Roskilde, Denmark) were coated overnight with 5 μg/ml antigen (50 μl/well) in 50 mM $NaHCO_3$ buffer (pH 9.6), washed, and blocked with buffer (0.05% Tween 20, 2% BSA in PBS) at room temperature for 2 h. The samples were serially diluted in PBS containing 0.05% Tween 20 (PBST), and the plates were then incubated for 1 h at 37°C. The plates were washed with PBST, incubated with the detecting antibody, and then developed using either PNPP or TMB-E.

For the avidity study, ricin-coated microtiter plates were incubated with anti-ricin antibodies (10 μg/ml) for 2 h, washed, and incubated with increasing concentrations of sodium thiocyanate (KSCN) for 10 min. After another wash step, the plates were incubated with alkaline phosphatase-conjugated anti-rabbit IgG, and the amount of bound antibody was determined. The results are expressed as the percentage of bound antibodies in the untreated wells.

**Affinity measurements.** Binding studies were carried out using the Octet RED system (ForteBio) that measures biolayer interferometry (BLI). All steps were performed at 30°C with shaking at 1,500 rpm in a 96-well plate containing 200 μl of solution in each well. Streptavidin-coated biosensors were loaded with biotinylated ricin (5 μg/ml) for 300 s, followed by a wash. The sensors were then reacted for 300 s with increasing concentrations of a ricin-purified fraction of antibodies and then moved to buffer-containing wells for another 300 s (dissociation phase). Binding and dissociation were measured as changes over time in light interference, and the curves were presented after the subtraction of parallel measurements from unloaded biosensors.

**Panning of phage libraries.** Three different phage display libraries were used: PhD-7, PhD-12, and PhD-C7C (New England BioLabs, MA). All the panning procedures were performed separately for each phage library, essentially as recommended by the kit's manufacturer. Briefly, affinity-purified antibodies (300 ng) were coincubated with 10 μl of stock phages for 20 min, and then the phage-antibody complexes were pulled down using protein G beads (alternating between magnetic- and agarose-based beads in each panning cycle). The beads were washed 10 times, and the phages were eluted using 0.2 M glycine-HCl (pH 2.2). The eluted phages were amplified in the kit-supplied *Escherichia coli*, precipitated in polyethylene glycol (PEG)-NaCl, and resuspended in PBS. The panning procedure was repeated for another two cycles, using the amplified stock of phages from the previous round of selection as the source for the next panning.

Individual clones from the third round of selection were selected and grown in 96-well plates. Each clone was then tested for its ability to specifically bind the polyclonal antibodies. Single-stranded DNA of the phage clones was prepared using BigDye (Applied Biosystems), and the PCR products were analyzed with the ABI Prism 310 genetic analyzer. The amino acids were deduced from the nucleotide codons to obtain the sequence of the selected peptides. The peptide sequences from the positive phages were aligned with the Clustal W software, and the crystal structure modeling was done using the PyMOL software.

**Protection from ricin intoxication.** Each mouse was anesthetized by an intraperitoneal (i.p.) injection of ketamine (1.9 mg/mouse) and xylazine (0.19 mg/mouse), and then antibodies at different doses (diluted in PBS) were applied intranasally. Twenty-four hours later, each mouse was anesthetized again, intoxicated intranasally with crude ricin (50 μl; 7 μg/kg of body weight diluted in PBS), and mortality was monitored over 14 days.

**Immunization of mice.** Primary immunization with selected phages was performed using a group of 5 mice by subcutaneous injections, each receiving a dose of $1 \times 10^7$ phages every 4 weeks. For the 1st injection, the phages were emulsified with complete Freund's adjuvant, while for the two booster injections, the phages were emulsified with incomplete Freund's adjuvant. The anti-ricin and anti-M13 titers of the vaccinated animals were monitored using an enzyme-linked immunosorbent assay (ELISA).

## RESULTS AND DISCUSSION

***In vitro* and *in vivo* ricin neutralization.** To characterize the antibody response to ricin toxoid immunization, we purified the IgG fraction from serum pooled from hyperimmune rabbits. The first step was to determine the neutralization potencies of these polyclonal antibodies *in vitro*. The common cell-based assays that measure ricin toxicity and are used to evaluate antibody-mediated neutralization measure cell survival at 48 to 72 h postintoxication (11, 14). However, since the ricin-mediated protein arrest is an early event that precedes cell death by many hours, we reasoned that accurate measurement at this step will allow us to shorten the assay without a loss of sensitivity. To this end, we used genetically engineered HEK293-AChE cells that were previously selected based upon their ability to constitutively synthesize and secrete large amounts of acetylcholinesterase (AChE) to the culture medium (26), and any changes in the enzyme level can be accurately measured. Indeed, the incubation of this cell line with increasing concentrations of ricin induced a significant and dose-responsive reduction of AChE in the culture medium, as determined 18 h after intoxication (Fig. 1A). The ricin concentration needed to

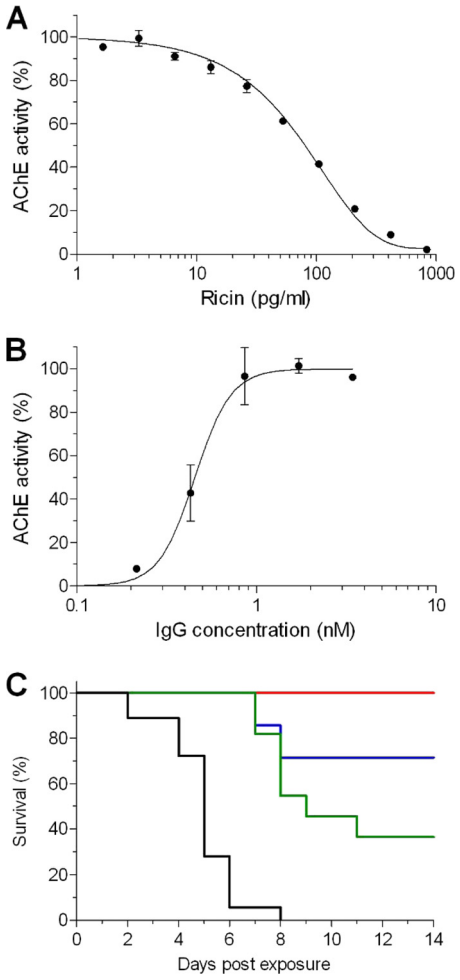


**FIG 1** *In vitro* and *in vivo* neutralization of ricin. (A) Cultured HEK293-AChE cells were incubated for 18 h with increasing concentrations of ricin. The residual AChE activity in the culture medium was determined and expressed as the percent activity determined for untreated cells. (B) Ricin (2 ng/ml) was mixed with increasing concentrations of the IgG fraction, the mixture was added to the cultured HEK293-AChE cells, and the residual AChE activity in the culture medium was determined 18 h later. (C) Mice were intranasally instilled with 3 μg (green line), 6.5 μg (blue line), or 13 μg (red line) of IgG. Twenty-four hours later, the mice were intranasally intoxicated with ricin (2× the $LD_{50}$), and animal survival was monitored for 14 days. Black line, intoxication control animals that were not pretreated with IgG. The data points are the means ± standard errors of the means (SEM) from triplicates.

reduce the levels of secreted AChE to 50% (50% inhibitory concentration [$IC_{50}$]) was determined to be 80 pg/ml.

The neutralizing efficacy of the polyclonal IgG preparation was studied next by coincubating ricin (at a concentration that induces a full protein synthesis arrest [2 ng/ml, 30 pM]) with increasing concentrations of antibodies before adding the antibody-toxin mixture to the 293-AChE cultured cells. As expected, the presence of the antibodies inhibited toxin activity and restored protein synthesis (Fig. 1B). The effective dose of antibodies needed to neutralize 50% ($ED_{50}$) of the toxin was 450 pM. It should be noted that the neutralizing antibody concentration at the $ED_{50}$ is in the nanomolar range, which is a property of very high-affinity antibodies.

These results have prompted us to determine the ability of this antibody preparation to protect mice from ricin intoxication. The mice were intranasally administered different doses of antibodies, and 24 h later, the animals were challenged with 2× the 50% lethal dose ($LD_{50}$) of ricin (7 μg/kg). All the animals in the control group (not pretreated with antibodies) succumbed within 8 days post-exposure (Fig. 1C). In contrast, 36% of the mice that were treated with 3 μg of anti-ricin antibodies survived the challenge, and a significant extension in the mean time to death (MTTD) was seen for the animals within this group that did not survive. Increasing the treatment doses to 6.5 μg and 13 μg resulted in 72% and 100% survival rates, respectively. These results are well correlated with the *in vitro* neutralization stoichiometric calculations, considering that ~5 μg of antibodies is needed to protect 50% of the mice that were intoxicated with 0.2 μg of ricin.

**Avidity and affinity of the anti-ricin antibodies.** To further appraise the antibody response following immunization with ricin toxoid, we measured IgG avidity. Antibody avidity (also termed functional affinity) is a binding parameter that characterizes the strength of the formed antibody-antigen complex (28). High avidity reflects the process of affinity maturation of the antibodies and was shown to be well correlated with higher neutralization titers toward several pathogens (29, 30). The avidity index (AI), which is the concentration of a chaotropic agent that yields a 50% reduction in the binding of antibody to antigen, is widely used to characterize and compare antibodies. Here, ricin-coated wells were preincubated with anti-ricin antibodies, the complex was exposed to increasing concentrations of the chaotropic agent (thiocyanate), and the reduction in the antibody binding to ricin was estimated. It was found that very high concentrations of the chaotropic agent were needed (>5 M) in order to affect the formed complex, and an AI value of 9 was calculated (Fig. 2A). This exceptionally high AI is a strong indicator for the formation of highly matured antibodies in response to ricin toxoid immunization.

We have also measured the affinity of the anti-ricin antibodies to ricin using the Octet RED biolayer interferometry system. In this system, the binding of molecules to the biosensor causes a wavelength shift in the interference pattern, which can be measured in real time. To determine the affinity constants in a more accurate manner, the specific ricin-binding antibodies were first isolated from the polyclonal IgG fraction by affinity chromatography. Biotinylated ricin was immobilized on the Octet sensor, and the binding profiles of the anti-ricin antibodies (at different concentrations) were monitored (Fig. 2B). It was found that although the assay was performed using polyclonal antibodies, the sensograms were fitted very well with a 1:1 binding model, with an apparent $K_D$ of 1.1 nM. This high-affinity value, which is an average of the sum of many individual antibody clones, indicates that in this population, there is a fraction of very high-affinity clones (below the nanomolar range).

**Immunological interaction with ricin subunits.** Our next goal was to determine the relative distribution of antibodies that recognize each of the two subunits of ricin. To this end, ELISA was performed using purified RTA or RTB as the coated antigen, and the apparent association constant ($K_A$) values were determined (Fig. 2C). By comparing these values to that obtained with native ricin ($K_A$, 0.35 $nM^{-1}$), we found that nearly 70% of the antibodies in the polyclonal serum recognize RTA ($K_A$, 0.23 $nM^{-1}$), while the remaining 30% of the antibodies recognize RTB ($K_A$, 0.11 $nM^{-1}$). Being a plant lectin, the ricin molecule carries plant-derived sugar

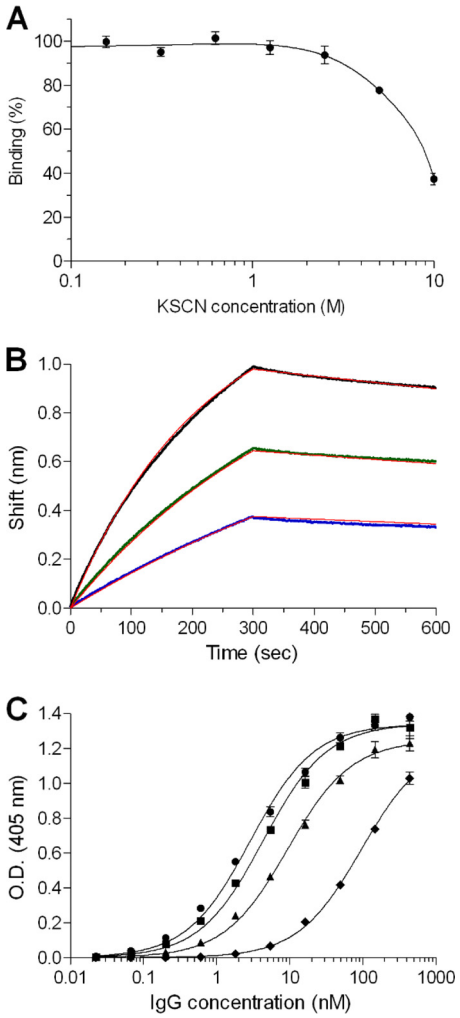


**FIG 2** Immunological characterization of the polyclonal antibodies to ricin. (A) The residual binding of preformed antibody-ricin complexes was measured following exposure to increasing concentrations of the KSCN chaotrope agent. (B) The affinity of ricin-specific antibodies was measured using biolayer interferometry. Biotinylated ricin was immobilized on a streptavidin biosensor and reacted for 300 s with increasing concentrations of antibodies (6.25 nM, blue line; 12.5 nM, green line; 25 nM, black line). The sensors were then immersed in buffer for another 300 s (dissociation phase). Red lines, curve fitting of 1:1 binding model. (C) Reactivity profile of the antibodies determined by ELISA using either ricin holotoxin (circles), RTA (squares), RTB (triangles) or *U. europaeus* (diamonds) as the antigens. The data points are the mean ± standard error of the mean (SEM) from triplicates. O.D., optical density.

moieties (in both subunits) that are known to be immunogenic, and it was of interest to determine the extent of the antibody response toward these sugar moieties. To address this question, we performed an ELISA using another plant lectin, *U. europaeus* (31), as the coated antigen. *U. europaeus* has no protein sequence homology to ricin but shares a similar pattern of sugar moieties, and indeed, a fraction of antibodies that recognize *U. europaeus* are present in the immunized rabbit sera (Fig. 2C). This fraction was estimated, however, to be no more than 3% of the total antibodies raised against ricin toxoid ($K_A$, 0.01 $nM^{-1}$).

**Identification of the immunodominant epitopes.** Identifying the B-cell epitopes in immunized serum is an important step in characterizing the humoral response to a given vaccine. Previous studies have identified several epitopes on ricin (neutralizing and nonneutralizing) (13). Most of these data were obtained using monoclonal antibodies, and some of it from mapping the immunodominant epitopes of polyclonal antibodies that were raised against RTA-based vaccines. We thus set out to identify the immunodominant epitopes in the sera of the rabbits that were immunized with ricin toxoid. The analysis was performed using three different phage display random peptide libraries containing either 7- or 12-mer linear peptides or cyclic 7-mer peptides that were panned against the affinity-purified fraction of the anti-ricin antibodies. Following three rounds, the amount of antibody-bound phages was enriched by a factor of 30, indicating successful panning. The clones that were eluted from the third round were individually verified for their ability to bind ricin and were subjected to sequence analysis. The most striking finding was that >70% of the antibody-binding phages, in all three libraries, contained the motif LPNR (Fig. 3). Moreover, about 50% from the 7-mer phages and all from the 12-mer phages shared a longer motif, PxLPNR. Based upon these results, a consensus sequence was deduced with the common motif aPxLPNRaxa, where "a" is either V, L, I, or M (hydrophobic residues). This motif fits very well with the RTA sequence $_{42}$IPVLPNRGLP$_{51}$ located in domain 1, and it is part of an exposed loop connecting helix A with β-sheet b, in close proximity to the enzymatic cleavage site of ricin (Fig. 4). Interestingly, this epitope was shown previously to be the exact target of a ricin-neutralizing monoclonal antibody (32).

The remaining phages were clustered into three additional epitopes (Fig. 3). Epitope 2 contained the consensus sequence PPSSQF, which matches exactly the sequence $_{262}$PPSSQF$_{267}$ in domain 3 of RTA, an exposed loop comprising the carboxylic end of this subunit (Fig. 4). Epitope 3 contained the motif SPIQxxR, which was represented in phages that were found in all three libraries and was best fitted to the RTA sequence $_{226}$FASPIQLQR$_{234}$, which is also located on domain 3 and is a part of a random coil (Fig. 4). The fourth epitope with the consensus sequence YWDGSI was the only epitope located on RTB, fitting the sequence $_{176}$YADGSI$_{181}$, which is part of the 2α subdomain that forms a loop that connects the two subdomains and is exposed to antibody interactions (Fig. 4).

The amount of phages associated with each epitope is probably a reflection of the distributions of their corresponding antibodies in the polyclonal serum. This however, does not necessary bear witness to the reactivity (affinity and neutralization) of each class of antibodies toward its cognate epitope. We therefore selected a representative phage from each group and examined its apparent affinity toward the polyclonal serum. The selected phages were those from the 7-mer library that shared the highest homology to ricin. Accordingly, epitope 1 was represented by the phage bearing the peptide sequence LPVLPNR, and the peptide sequences of the phages for the rest of the epitopes are marked in Fig. 4. It was found that the apparent affinity of epitope 1, the major immunodominant epitope, was the highest (as determined by the half-maximum binding; Fig. 5A), and the next best binder was found to be epitope 4. The binding of the polyclonal serum to these epitopes was also verified using synthetic peptides (data not shown).

**Involvement of the immunodominant epitopes in ricin neutralization.** The cumulative findings so far regarding the potency of the IgG preparation and the identification of the immunodom-

| | Sequence | Library | Frequency |
|---|---|---|---|
| **Epitope 1** | a**P**a**LPNR** | 7 mer | 13 |
| | a**P**x**LPNR** | " | 23 |
| | x**P**a**LPNR** | " | 7 |
| | x**P**x**LPNR** | " | 4 |
| | axx**LPNR** | " | 1 |
| | xxa**LPNR** | " | 2 |
| | xxx**LPNR** | " | 1 |
| | a**LPNR**ax | " | 5 |
| | x**LPNR**ax | " | 1 |
| | x**LPNR**xx | C7C mer | 1 |
| | **LPNR**axx | " | 4 |
| | **LPNR**xxx | " | 4 |
| | x**P**x**LPNR** | " | 4 |
| | xxx**LPNR** | " | 4 |
| | xxxx**PNR** | " | 4 |
| | **LPNR**axa | " | 3 |
| | **LPNR**axx | " | 5 |
| | **LPNR**xxa | " | 5 |
| | **LPNR**xxx | " | 3 |
| | xxx**P**x**LPNR**xxx | 12 mer | 9 |
| | xa**P**x**LPNR**xxxx | " | 13 |
| | a**P**x**LPNR**xxxxx | " | 1 |
| Consensus: | **aPxLPNRaxa** | | |
| RTA 42-51: | IPVLPNRVGLP | | |
| **Epitope 2** | G**PPSSQF*** | 7 mer | 1 |
| | M**PPSHQF** | " | 1 |
| | I**P**L**SSQF** | " | 1 |
| | L**P**L**S**N**Q**L | " | 1 |
| | M**PP**F**S**NL | " | 1 |
| | M**P**W**L**S**N**F | " | 1 |
| | PITNA**PSHQF** | 12 mer | 1 |
| Consensus: | **PPSSQF** | | |
| RTA 258-267: | RCAPPPSSQF | | |
| **Epitope 3** | **SPIQAHR*** | 7 mer | 1 |
| | **SPIQCSR** | " | 1 |
| | **SPNQCSR** | " | 1 |
| | QVFV**SPIQAHR** | 12 mer | 1 |
| Consensus: | **SPIQxxR** | | |
| RTA 224-234: | GAFASPIQLQR | | |
| **Epitope 4** | **YWDGSIQ*** | 7 mer | 1 |
| | S**YWDRSI** | 7 mer | 1 |
| | AWR**DGSI** | 7 mer | 1 |
| Consensus: | **YWDGSI** | | |
| RTB 175-182: | LYADGSIR | | |

**FIG 3** Sequence alignment of the phage-derived peptides selected by panning with anti-ricin antibodies. Three rounds of panning were performed using random peptide phage display libraries (7- or 12-mer linear peptides and 7-mer constrained peptides). The peptide sequences of the phages that specifically bound the antibodies were deduced and divided into four groups based upon multiple alignment. The frequency (no.) of peptides in each group is indicated. The consensus amino acids are highlighted in bold. The hydrophobic amino acids (V, L, I, or M) within the peptides are indicated by "a," where "x" represents sites with no amino acid homology. The underlined amino acids represent those with full homology to ricin. The peptides that were taken as representatives of their epitope group are marked with an asterisk.

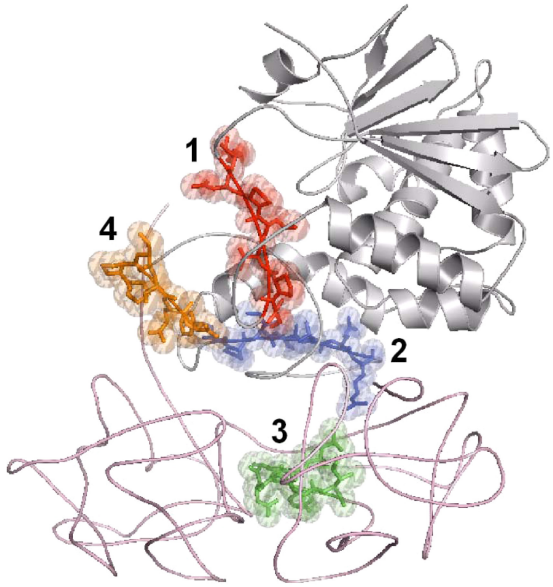


**FIG 4** Modeling of the immunodominant epitopes on ricin. Crystal structure of ricin (PDB 2AAI; RTA in gray and RTB in pink) emphasizing the locations of epitope 1 (red), epitope 2 (blue), epitope 3 (green), and epitope 4 (orange).

inant epitopes raise the question of whether we can determine which of these epitopes are important for ricin neutralization. Our working hypothesis was that the incubation of ricin-neutralizing antibodies with phages that mimic their cognate epitope will compete in binding to the toxin and consequently inhibit the ability of this subset of antibodies to neutralize ricin. In order to increase the sensitivity of this assay, we have used the minimal concentration of antibodies that is needed to neutralize 95% of the ricin toxicity toward cultured cells. Each representative phage was preincubated with the antibodies at its highest possible concentration before it was mixed with ricin and added to the cell culture. Under these conditions, the preclusion of the neutralizing antibodies from binding to ricin will allow the toxin to induce protein synthesis arrest. Twenty-four hours later, the residual activity of AChE in the culture medium was determined and compared to that of the control (antibodies without phages). Incubating the antibodies with a nonspecific (NS) phage did not affect their neutralizing activities (Fig. 5B). However, incubating the antibodies with the phage representing epitope 1 resulted in a marked inhibition of 30% of the antibody activity. A similar effect was achieved when the phage representing epitope 4 (located on RTB) was added to the assay. The presence of the phages representing epitopes 2 and 3 also reduced serum-neutralizing activity, albeit to a much lesser extent (~10%), which was not significantly different. We have also tested a mixture of several phages but did not see a beneficial effect, probably since the effective concentration of each phage was lower.

The observation that epitope 1 has a role in ricin neutralization is in agreement with a previous report that demonstrated that this epitope is the target of an anti-ricin monoclonal antibody (32). In line with this, epitopes 2 and 3, which were not as effective in neutralizing ricin, are located in the so-called ricin-immunodominant regions V and VI, respectively, which are the targets of non-neutralizing antibodies (24). The binding site on the RTB subunit that comprises epitope 4, on the other hand, was not reported before, and the fact that it is the target for neutralizing antibodies might have broader implications for understanding ricin activity. The RTB subunit mediates the binding of the toxin to the target cell via two globular subdomains (1α and 2γ). Once internalized, RTB interacts with intracellular components to further mediate retrograde trafficking to the endoplasmic reticulum (ER) compartment by an unknown mechanism. The modeling of epitope 4 on the crystal structure of ricin reveals that it is spatially located

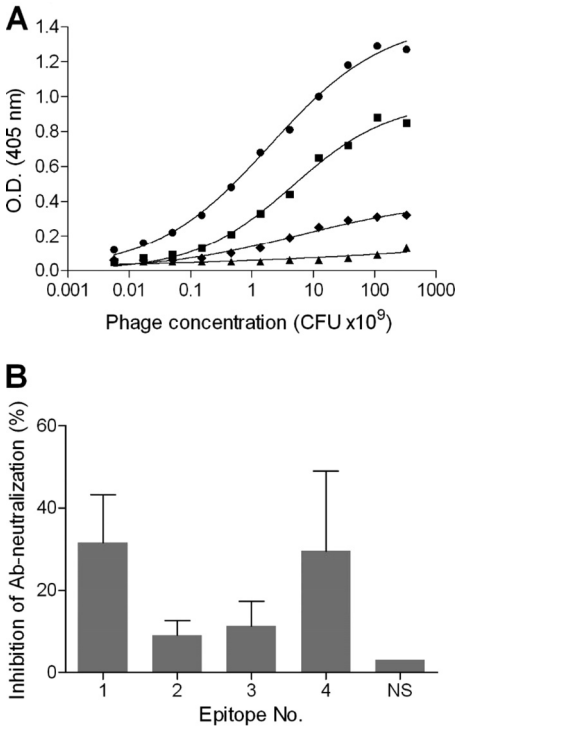


**FIG 5** Interaction of selected phage clones with anti-ricin antibodies. (A) ELISA plate was coated with anti-ricin antibodies, followed by the addition of a serially diluted representative phage clone from each group of epitopes (circles, epitope 1; triangles, epitope 2; diamonds, epitope 3; squares, epitope 4). Bound phages were then detected using anti-M13 antibodies, and results shown are from a representative experiment. (B) A fixed amount of ricin and antibodies were preincubated with a representative phage clone from each group of epitopes. The mixture was then added to the HEK293-AChE cells, and the secreted AChE activity was determined 18 h later. The results are expressed as the percent total inhibition of antibody (Ab)-neutralizing activity in the absence of phages. NS, nonspecific phage. The presented data are the mean ± SEM from triplicates.

between the two subdomains of RTB, considerably distant from the two galactose binding pockets, suggesting that this epitope is not directly involved in the binding of the toxin to target cell surfaces. Interestingly, this epitope is part of a highly conserved hydrophobic core (found on both subdomains) that also can be found in the sequence of the ricin agglutinin B (33). Taken together, our results imply that this epitope may have a role in ricin toxicity other than in binding to target cells, such as enabling downstream interactions with retrograde-related proteins. Deciphering the role of this region is beyond the scope of the current study; however, it encourages further investigation using molecular biology tools and mutated toxin derivatives.

**Immunogenic properties of the selected immunodominant epitopes.** As antigenic mimics, it can be expected that the selected phage-bearing epitopes will induce an immune response that will cross-react with ricin, as has been demonstrated for other antigens (19). To test this hypothesis, mice were immunized with each phage that represents the four immunodominant epitopes. Indeed, it was found that animals in all four groups developed a significant anti-ricin response (Fig. 6), indicating that the selected peptides are indeed good mimics of ricin B-cell epitopes.

**Conclusions.** We characterized the polyclonal antibody response toward holotoxin ricin-based vaccination, identified four

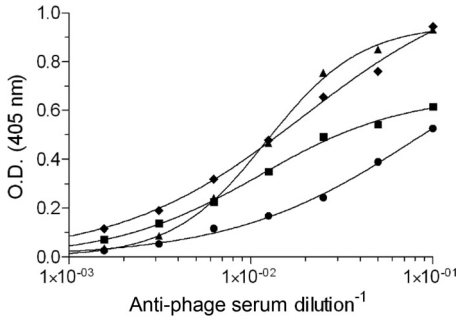


**FIG 6** Cross-reactivity of anti-phage antibodies and ricin. Mice ($n = 5$) were immunized with a representative phage clone from each group of epitopes (circles, epitope 1; triangles, epitope 2; diamonds, epitope 3; squares, epitope 4). The reactivities of the antibodies that were raised against these phages were determined by ELISA using ricin as the coated antigen. The results are from a representative mouse from each vaccinated group or a naive mouse.

immunodominant epitopes, and determined which of these epitopes are relevant to toxin neutralization. These four epitopes, even when presented on the surface of a filamentous phage, induced a cross-reactive response of antibodies that recognize ricin. To the best of our knowledge, this is the first time that epitope mapping of the polyclonal response following immunization with ricin holotoxin was performed. As there is an ongoing effort by health and defense organizations all over the world to develop an effective vaccine against ricin, we believe that the findings of this study will provide useful information and a possible strategy for designing an improved vaccine to this toxin.

## REFERENCES

1. **Olsnes S, Kozlov JV.** 2001. Ricin. Toxicon. **39:**1723–1728. http://dx.doi.org/10.1016/S0041-0101(01)00158-1.
2. **Bai Y, Watt B, Wahome PG, Mantis NJ, Robertus JD.** 2010. Identification of new classes of ricin toxin inhibitors by virtual screening. Toxicon **56:**526–534. http://dx.doi.org/10.1016/j.toxicon.2010.05.009.
3. **Miller DJ, Ravikumar K, Shen H, Suh JK, Kerwin SM, Robertus JD.** 2002. Structure-based design and characterization of novel platforms for ricin and Shiga toxin inhibition. J. Med. Chem. **45:**90–98. http://dx.doi.org/10.1021/jm010186s.
4. **Hesselberth JR, Miller D, Robertus J, Ellington AD.** 2000. *In vitro* selection of RNA molecules that inhibit the activity of ricin A-chain. J. Biol. Chem. **275:**4937–4942. http://dx.doi.org/10.1074/jbc.275.7.4937.
5. **Nagatsuka T, Uzawa H, Ohsawa I, Seto Y, Nishida Y.** 2010. Use of lactose against the deadly biological toxin ricin. ACS Appl. Mater. Interfaces **2:**1081–1085. http://dx.doi.org/10.1021/am900846r.
6. **Stechmann B, Bai SK, Gobbo E, Lopez R, Merer G, Pinchard S, Panigai L, Tenza D, Raposo G, Beaumelle B, Sauvaire D, Gillet D, Johannes L, Barbier J.** 2010. Inhibition of retrograde transport protects mice from lethal ricin challenge. Cell **141:**231–242. http://dx.doi.org/10.1016/j.cell.2010.01.043.
7. **Smallshaw JE, Vitetta ES.** 2011. Ricin vaccine development. Curr. Top. Microbiol. Immunol. **357:**259–272. http://dx.doi.org/10.1007/82_2011_156.
8. **Maddaloni M, Cooke C, Wilkinson R, Stout AV, Eng L, Pincus SH.** 2004. Immunological characteristics associated with the protective efficacy of antibodies to ricin. J. Immunol. **172:**6221–6228. http://dx.doi.org/10.4049/jimmunol.172.10.6221.
9. **Pincus SH, Das A, Song K, Maresh GA, Corti M, Berry J.** 2014. Role of Fc in antibody-mediated protection from ricin toxin. Toxins (Basel) **6:**1512–1525. http://dx.doi.org/10.3390/toxins6051512.
10. **Pratt TS, Pincus SH, Hale ML, Moreira AL, Roy CJ, Tchou-Wong KM.** 2007. Oropharyngeal aspiration of ricin as a lung challenge model for evaluation of the therapeutic index of antibodies against ricin A-chain for post-exposure treatment. Exp. Lung Res. **33:**459–481. http://dx.doi.org/10.1080/01902140701731805.
11. **Vance DJ, Tremblay JM, Mantis NJ, Shoemaker CB.** 2013. Stepwise

engineering of heterodimeric single domain camelid VHH antibodies that passively protect mice from ricin toxin. J. Biol. Chem. **288:**36538–36547. http://dx.doi.org/10.1074/jbc.M113.519207.
12. **Gal Y, Mazor O, Alcalay R, Seliger N, Aftalion M, Sapoznikov A, Falach R, Kronman C, Sabo T.** 2014. Antibody/doxycycline combined therapy for pulmonary ricinosis: attenuation of inflammation improves survival of ricin-intoxicated mice. Toxicol. Rep. **1:**496–504. http://dx.doi.org/10.1016/j.toxrep.2014.07.013.
13. **O'Hara JM, Yermakova A, Mantis NJ.** 2011. Immunity to ricin: fundamental insights into toxin-antibody interactions. Curr. Top. Microbiol. Immunol. **357:**209–241. http://dx.doi.org/10.1007/82_2011_193.
14. **Prigent J, Panigai L, Lamourette P, Sauvaire D, Devilliers K, Plaisance M, Volland H, Créminon C, Simon S.** 2011. Neutralising antibodies against ricin toxin. PLoS One **6:**e20166. http://dx.doi.org/10.1371/journal.pone.0020166.
15. **Yermakova A, Mantis NJ.** 2011. Protective immunity to ricin toxin conferred by antibodies against the toxin's binding subunit (RTB). Vaccine **29:**7925–7935. http://dx.doi.org/10.1016/j.vaccine.2011.08.075.
16. **Mason JT, O'Leary TJ.** 1991. Effects of formaldehyde fixation on protein secondary structure: a calorimetric and infrared spectroscopic investigation. J. Histochem. Cytochem. **39:**225–229. http://dx.doi.org/10.1177/39.2.1987266.
17. **Kende M, Yan C, Hewetson J, Frick MA, Rill WL, Tammariello R.** 2002. Oral immunization of mice with ricin toxoid vaccine encapsulated in polymeric microspheres against aerosol challenge. Vaccine **20:**1681–1691. http://dx.doi.org/10.1016/S0264-410X(01)00484-4.
18. **Buchwald UK, Lees A, Steinitz M, Pirofski LA.** 2005. A peptide mimotope of type 8 pneumococcal capsular polysaccharide induces a protective immune response in mice. Infect. Immun. **73:**325–333. http://dx.doi.org/10.1128/IAI.73.1.325-333.2005.
19. **De Berardinis P, Sartorius R, Fanutti C, Perham RN, Del Pozzo G, Guardiola J.** 2000. Phage display of peptide epitopes from HIV-1 elicits strong cytolytic responses. Nat. Biotechnol. **18:**873–876. http://dx.doi.org/10.1038/78490.
20. **Meloen RH, Puijk WC, Slootstra JW.** 2000. Mimotopes: realization of an unlikely concept. J. Mol. Recognit. **13:**352–359. http://dx.doi.org/10.1002/1099-1352(200011/12)13:6<352::AID-JMR509>3.0.CO;2-C.
21. **Pashov A, Canziani G, Monzavi-Karbassi B, Kaveri SV, Macleod S, Saha R, Perry M, Vancott TC, Kieber-Emmons T.** 2005. Antigenic properties of peptide mimotopes of HIV-1-associated carbohydrate antigens. J. Biol. Chem. **280:**28959–28965. http://dx.doi.org/10.1074/jbc.M502964200.
22. **Siman-Tov DD, Navon-Perry L, Haigwood NL, Gershoni JM.** 2006. Differentiation of a passive vaccine and the humoral immune response toward infection: analysis of phage displayed peptides. Vaccine **24:**607–612. http://dx.doi.org/10.1016/j.vaccine.2005.08.039.
23. **Castelletti D, Fracasso G, Righetti S, Tridente G, Schnell R, Engert A, Colombatti M.** 2004. A dominant linear B-cell epitope of ricin A-chain is the target of a neutralizing antibody response in Hodgkin's lymphoma patients treated with an anti-CD25 immunotoxin. Clin. Exp. Immunol. **136:**365–372. http://dx.doi.org/10.1111/j.1365-2249.2004.02442.x.
24. **O'Hara JM, Neal LM, McCarthy EA, Kasten-Jolly JA, Brey RN, III, Mantis NJ.** 2010. Folding domains within the ricin toxin A subunit as targets of protective antibodies. Vaccine **28:**7035–7046. http://dx.doi.org/10.1016/j.vaccine.2010.08.020.
25. **National Institutes of Health.** 1996. Guide for the care and use of laboratory animals. National Academy Press, Washington, DC.
26. **Kronman C, Velan B, Gozes Y, Leitner M, Flashner Y, Lazar A, Marcus D, Sery T, Grosfeld H, Cohen S, Shafferman A.** 1992. Production and secretion of high levels of recombinant human acetylcholinesterase in cultured cell lines: microheterogeneity of the catalytic subunit. Gene **121:**295–304. http://dx.doi.org/10.1016/0378-1119(92)90134-B.
27. **Ellman GL, Courtney KD, Andres V, Jr, Featherstone RM.** 1961. A new and rapid colorimetric determination of acetylcholinesterase activity. Biochem. Pharmacol. **7:**88–95. http://dx.doi.org/10.1016/0006-2952(61)90145-9.
28. **Macdonald RA, Hosking CS, Jones CL.** 1988. The measurement of relative antibody affinity by ELISA using thiocyanate elution. J. Immunol. Methods **106:**191–194. http://dx.doi.org/10.1016/0022-1759(88)90196-2.
29. **Boxus M, Lockman L, Fochesato M, Lorin C, Thomas F, Giannini SL.** 2014. Antibody avidity measurements in recipients of Cervarix vaccine following a two-dose schedule or three-dose schedule. Vaccine **32:**3232–3236. http://dx.doi.org/10.1016/j.vaccine.2014.04.005.
30. **Longworth E, Borrow R, Goldblatt D, Balmer P, Dawson M, Andrews N, Miller E, Cartwright K.** 2002. Avidity maturation following vaccination with a meningococcal recombinant hexavalent PorA OMV vaccine in UK infants. Vaccine **20:**2592–2596. http://dx.doi.org/10.1016/S0264-410X(02)00151-2.
31. **Audette GF, Vandonselaar M, Delbaere TJ.** 2000. The 2.2 A resolution structure of the O(H) blood-group-specific lectin I from *Ulex europaeus*. J. Mol. Biol. **304:**423–433. http://dx.doi.org/10.1006/jmbi.2000.4214.
32. **Dai J, Zhao L, Yang H, Guo H, Fan K, Wang H, Qian W, Zhang D, Li B, Wang H, Guo Y.** 2011. Identification of a novel functional domain of ricin responsible for its potent toxicity. J. Biol. Chem. **286:**12166–12171. http://dx.doi.org/10.1074/jbc.M110.196584.
33. **Rutenber E, Robertus JD.** 1991. Structure of ricin B-chain at 2.5 A resolution. Proteins **10:**260–269. http://dx.doi.org/10.1002/prot.340100310.